Investigating the Role of Neck Muscle Activation and Neck Damping Characteristics in Brain Injury Mechanism

Hossein Bahreinizad[1], Suman K. Chowdhury[1*]

[1]Department of Industrial, Manufacturing and Systems Engineering, Texas Tech University, Lubbock, Texas, USA

*All correspondence should be addressed to—

Dr. Suman K. Chowdhury, Assistant Professor, Department of Industrial, Manufacturing and Systems Engineering, Texas Tech University

905 Canton Ave, Lubbock 79409-3061, Texas, USA.

. E-mail: suman.chowdhury@ttu.edu; Tel: +1 (806)-834-7908.

ORCID: 0000-0001-8567-1759

Acknowledgements

This work was primarily supported by the National Science Foundation (**2239110**). We thank Felipe Santos, Leonardo Wei, and Gustavo Paulon for their assistance in data processing and finite element model development.

Abstract

Purpose: This study aimed to investigate the role of neck muscle activity and neck damping characteristics in traumatic brain injury (TBI) mechanisms.

Methods: We used a previously validated head-neck finite element (FE) model that incorporates various components such as scalp, skull, cerebrospinal fluid, brain, muscles, ligaments, cervical vertebrae, and intervertebral discs. Impact scenarios included a Golf ball impact, NBDL linear acceleration, and Zhang's linear and rotational accelerations. Three muscle activation strategies (no-activation, low-to-medium, and high activation levels) and two neck damping levels by perturbing intervertebral disc properties (high: hyper-viscoelastic and low: hyper-elastic) strategies were examined. We employed Head Injury Criterion (HIC), Brain Injury Criterion (BrIC), and maximum principal strain (MPS) as TBI measures.

Results: Increased neck muscle activation consistently reduced the values of all TBI measures in Golf ball impact (HIC: 4%-7%, BrIC: 11%-25%, and MPS (occipital): 27%-50%) and NBDL study (HIC: 64%-69%, BrIC: 3%-9%, and MPS (occipital): 6%-19%) simulations. In Zhang's study, TBI metric values decreased with the increased muscle activation from no-activation to low-to-medium (HIC: 74%-83%, BrIC: 27%-27%, and MPS (occipital): 60%-90%) and then drastically increased with further increases to the high activation level (HIC: 288%-507%, BrIC: 1%-25%, and MPS (occipital): 23%-305%). Neck damping changes from low to high decreased all values of TBI metrics, particularly in Zhang's study (up to 40% reductions).

Conclusion: Our results underscore the pivotal role of neck muscle activation and neck damping in TBI mitigation and holds promise to advance effective TBI prevention and protection strategies for diverse applications.

Keywords: Simulation and modeling, Finite element method, Traumatic brain injury, Computational biomechanics, Neck damping, Active muscles

Statements and Declarations

The authors have no competing interest to declare.

Introduction

Traumatic brain injury (TBI) occurs when a sudden mechanical impact to the head or body leads to structural and functional changes in the brain [1]. According to the Global Burden of Diseases, Injuries, and Risk Factors (GBD) report, the prevalence of TBI increased by 24.4% from 1990 to 2019, with an estimated 49 million cases globally in 2019. In the United States alone, the Centers for Disease Control and Prevention Wonder database reported 69,473 TBI-related deaths in 2021 and 223,135 TBI-related hospitalizations in 2019 [2]. The leading causes of TBI are falls, followed by motor vehicle accidents, assault, and firearm-related injuries [3-5]. Sports (e.g., football, hockey, etc.) and recreational activities (e.g., bicycling, horse riding, and playground activities) are also major causes of TBIs [6, 7]. According to a 2019 CDC report approximately 283,000 children (under the age of 18) visited the emergency department due to TBIs associated with sports and recreational activities [8]. Previous TBI studies have identified the unrestricted, rapid acceleration of the head as the main factor contributing to TBIs [9, 10]. This rapid head motion, primarily governed by the action of neck muscles, is also influenced by the neck damping characteristics, which stem primarily from the cervical intervertebral discs and ligaments [11, 12]. Thus, in order to develop effective preventive measures, it is crucial to investigate how neck muscles and neck damping characteristics influence the TBI mechanism, i.e., the rapid deformation and strain of the brain.

Previous literature showed a range of experimental (both in-vivo and in-vitro studies) and computational methods to study the TBI mechanism. In-vivo experimental studies primarily utilized quantitative video analysis [13] and wearable sensors [14] to understand the injury characteristics and TBI mechanisms based on head kinematics. However, these approaches are limited in their ability to measure internal parameters of the brain and other head components. On the other hand, in-vitro experimental studies used anthropometric test device [15] and/or cadavers [16], to explore the mechanical response of internal head components. Nevertheless, both experimental approaches may not fully capture the complexities of the living human body. To overcome these limitations of experimental methods, researchers have turned to computational approaches in TBI research. Notably, finite element (FE) models have gained popularity as powerful tools for studying TBI. These models can offer a highly detailed representations of the biomechanical behavior of head and neck structures, enabling the study of both external kinematics and internal responses of the brain and other head components during various impact scenarios [11, 12, 17, 18]. Thus, by leveraging FE-based head-neck computational models, researchers can overcome the limitations of experimental methods and gain a more comprehensive understanding of TBI mechanics and associated preventive measures.

In general, cervical intervertebral discs acts as damper in the head-neck system, thereby absorbing the impact forces and reducing the risk of brain and other head-neck injuries [19]. Furthermore, the surrounding neck muscles play a crucial role in

counteracting the external forces and mitigating the injury severity of the head-neck system [20]. Neck muscles also exert compressive forces to counteract the tensile force induced by the external impact forces acting on the head-neck system. The direction and magnitude of these compressive forces depend on individual neck muscles' maximum strength, activation level, position, and their roles a flexor, extensor, or rotator muscle [21]. Accordingly, some experimental studies investigated the role of neck muscles in reducing the head-neck injury severity, however, they reported conflicting findings – Some studies [22, 23] found a significant reduction in TBI risk associated with increased neck muscle strength, whereas other studies [24-26] reported no significant effect. To address these putative results, Jin et al. [11] employed a computational head-neck model to investigate the impact of neck muscle activation levels and strategies on brain injury mechanism. They observed that though an increased muscle activation level reduces the brain injury risk, the combined muscle activation strategies had a more significant effect on it. In another head-neck FE study by Bruneau et al. [17], the increased muscle activation was found to cause reduced head-neck kinematics. However, both these studies [11, 17] did not consider the influence of neck damping characteristics. On the contrary, Dirisila et al. [12] investigated the influence of neck damping on the brain response to a direct frontal impact to the head using a rigid impactor and modeled the neck as a simple spring-damper system (instead of modeling biofidelic cervical vertebrae, muscles, intervertebral discs, and ligaments) in their head-neck FE model. Their observations indicated that neck damping, characterized by viscoelastic properties, had minimal effects on the brain response in the initial stages (simulation time) of an impact but subsequently reduced the brain's stress response in the later stages of the impact. Findings of these studies highlight the necessity of further research on the development of a FE model incorporating accurate neck muscle activation strategies and damping properties of intervertebral discs, in addition to explore how neck muscle activation and neck damping properties can collectively affect the TBI mechanism.

Therefore, the goal of this study was to explore the role of neck muscle activity and neck damping characteristics in TBI mechanism. Specifically, we aimed to assess the effects of various muscle activation strategies (no activation, low/medium activation, and high activation) and neck damping properties (hyper-viscoelastic/hyper-elastic intervertebral disks) on the mechanical response of the head-neck system under various impact scenarios, including Golf ball impacts, linear acceleration, and combined linear and rotational acceleration. By conducting these simulations, we seek to gain a comprehensive understanding of the mechanisms underlying TBI protection and provide insights for the development of effective preventive strategies. This research has the potential to enhance our knowledge of the neck's role in mitigating brain injuries and contribute to improved safety measures in impact-related activities.

Materials and Methods

Head-neck model

We used our previously validated head-neck FE model to investigate our study objective [27]. The model incorporates various components, including the scalp, skull, cerebrospinal fluid (CSF), brain, dura mater, pia mater, neck muscles, neck ligaments, cervical vertebrae (C1-C7), and intervertebral discs [27]. This model was created using head and neck MRI data derived from a male participant (age: 42 years, height: 176 cm, and weight: 106 kg), resulting in a comprehensive structure comprising 1.36 million elements. In this model, the scalp, skull, and neck segments contributed 0.27 million, 0.23 million, and 0.072 million tetrahedral elements, respectively. Additionally, the model featured 0.1 million quad shell elements, with the dura and pia maters accounting for 0.05 million and 0.04 million elements, respectively. We modeled the skull, pia mater, dura mater, and vertebrae as linear elastic materials. The scalp was represented using a linear viscoelastic material, the CSF as a hyper-elastic material, the intervertebral discs as hyper-viscoelastic materials, and the brain's gray and white matter as a hyper-viscoelastic material. One notable feature of this model is its incorporation of the Hill-type muscle model [28], allowing us to simulate active muscle behavior and investigate the impacts of muscle activation on our study objectives. Moreover, we modeled the intervertebral discs with a hyper-viscoelastic material model [29]. The material properties of individual head-neck structures are provided in Table 1 [27].

Table 1 Material properties and constitutive equations of each head-neck structure included in our model.

Segment	Material model	Material constants	Constitutive Equation
Scalp [30]	Linear viscoelastic	$G_0 = 1.70\ MPa, G_\infty = 0.68\ MPa$ $K = 20\ MPa$ $\beta = 0.00003$ $\rho = 1100\ kg/m^3$	$G(t) = G_\infty + (G_0 - G_\infty)e^{-\beta t}$
Skull [31]	Linear elastic	$E = 15.00\ GPa$ $\rho = 1800\ kg/m^3$ $v = 0.21$	$\sigma = E\varepsilon$
Dura mater [32]	Linear elastic	$E = 5.00\ MPa$ $\rho = 1200\ kg/m^3$ $v = 0.45$	$\sigma = E\varepsilon$
Pia mater [32]	Linear elastic	$E = 2.30\ GPa$ $\rho = 1000\ kg/m^3$ $v = 0.45$	$\sigma = E\varepsilon$
Vertebrae [33]	Linear elastic	$E = 8.00\ GPa$ $\rho = 1200\ kg/m^3$ $v = 0.22$	$\sigma = E\varepsilon$
CSF [34]	Hyper-elastic	$C_{10} = 0.0112$ $\rho = 1000\ kg/m^3$ $v = 0.499$	$W(J_1, J_2, J) = \sum_{p,q=0}^{n} C_{pq}(J_1 - 3)^p (J_2 - 3)^q + W_H(J)$
White matter [35, 36]	Hyper-viscoelastic	$\mu_0 = 1.18\ kPa, \alpha = -4.77$ $\rho = 1060\ kg/m^3$ $v = 0.4977$ $g_1 = 0.653$ $g_2 = 0.206\ M$ $\tau_1 = 0.448\ s, \tau_2 = 15.007\ s$	$W = \frac{2\mu_0}{\alpha^2}\left(\bar{\lambda}_1^\alpha + \bar{\lambda}_2^\alpha + \bar{\lambda}_3^\alpha - 3\right)$ $\mu = \mu_0\left[1 - \sum_{i=1}^{2} g_i(1 - e^{-t/\tau_i})\right]$
Grey matter [35, 36]	Hyper-viscoelastic	$\mu_0 = 0.84\ kPa, \alpha = -4.77$ $\rho = 1060\ kg/m^3$ $v = 0.4977$ $g_1 = 0.653$ $g_2 = 0.206\ M$ $\tau_1 = 0.448\ s, \tau_2 = 15.007\ s$	$W = \frac{2\mu_0}{\alpha^2}\left(\bar{\lambda}_1^\alpha + \bar{\lambda}_2^\alpha + \bar{\lambda}_3^\alpha - 3\right)$ $\mu = \mu_0\left[1 - \sum_{i=1}^{2} G_i(1 - e^{-t/\tau_i})\right]$
Intervertebral discs [37]	Hyper-viscoelastic	$C_{10} = 0.15, C_{01} = 0.03$ $\rho = 1000\ kg/m^3$ $v = 0.499$ $G_1 = 1.70, G_2 = 1.20, G_3 = 2.00$ $\tau_1 = 11.76, \tau_2 = 1.10, \tau_3 = 0.13$	$W(J_1, J_2, J) = \sum_{p,q=0}^{n} C_{pq}(J_1 - 3)^p (J_2 - 3)^q + W_H(J)$ $G(t) = \sum_{k=1}^{n} G_k exp^{-t/\tau_k}$
Muscles [38, 39]	Hill-type	PCSA [38] Muscle volume [38]	$F_{active} = F_{max} \times f_{FL} \times f_{FV} \times A(t)$ $F_{Passive} = \frac{F_{max}}{e^{K_{sh}} - 1}\left[e^{\frac{K_{sh}}{L_{max}}\left(\frac{L}{L_{rest}} - 1\right)} - 1\right]\ For\ L > L_{rest}$
Ligaments [40]	Linear spring	k [40]	$F = kx$

E: Elastic modulus, G_0: short-term shear modulus, G_∞: long-term shear modulus, K: bulk modulus, β: decay constant, ρ: density, v: Poisson ratio, τ_k: relaxation time, g_k: relaxation coefficient, $\bar{\lambda}_i^\alpha$: principal stretch, W: strain energy density function, C_{pq}, μ: shear modulus, α: material constants, F_{active}: active muscle force, $F_{passive}$: passive muscle force, f_{FL} : force-length relation of the muscle, f_{FV}: force-velocity relation of the muscle, A(t): muscle's activation level versus time relationship, L_{rest} : the resting length and K_{sh} : passive muscle force constant, k: ligament stiffness.

Impact Loads

We simulated three impact conditions (Fig. 1). To address the roles played by the neck under focal injury conditions (confined to brain damage at one specific area), we simulated a Golf ball impact scenario, as outlined in a previous study [41]. Our simulation included a Golf ball hitting the frontal area of the head model with an initial velocity of 35 m/s. The Golf ball was represented as a three-layered structure consisting of an inner core, a mantle, and a cover. The core and mantle were modeled using hyper-viscoelastic materials, while the cover was modeled using a hyper-viscoelastic material (Table 2) [3]. Equation 1 describes the hyper-elastic behavior of Golf ball layers, whereas Equation 2 describes their viscoelastic response.

$$W(I_1, I_2) = C_{10}(J_1 - 3) + C_{01}(J_2 - 3) \quad (1)$$

$$G(t) = \sum_{j=1}^{n} G_j e^{-\beta_j t} \quad (2)$$

In Equations 1 and 2, *J* is invariant of the right Cauchy-Green deformation tensor, W is the strain energy density function, β is the decay constant, G_j is the shear relaxation modulus, G is shear modulus for frequency independent damping and SIGF is the stress limit for frequency independent damping. We connected the Golf ball's three layers using a tied boundary condition.

Our second and third impact scenarios were carefully selected to investigate the role of neck in diffuse injuries, which involve more extensive disruption of brain tissue and can affect multiple areas simultaneously [9, 10, 44]. As diffuse injuries are primarily associated with acceleration scenarios [10], we incorporated two acceleration scenarios: 1) the linear acceleration scenario from the Naval Biodynamics Laboratory (NBDL) study [45] and 2) the combined linear and rotational acceleration scenario proposed by Zhang et al. [43]. The NBDL acceleration profile was applied to the entire head-neck model, while the Zhang's acceleration profile specifically targeted the center of mass of the head. The Zhang's acceleration scenario was derived from the recreation of American football accidents. Considering the ongoing debate surrounding the main cause of injuries, whether it is linear or rotational acceleration, it was imperative for us to include both scenarios in our study.

Table 2 Mechanical characteristics of the Golf ball [3].

	Outer diameter (mm)	No. of elements	ρ (kg/m^3)	ν	C_{01} (MPa)	C_{10} (MPa)	G_1 (MPa)	β_1 (S^{-1})	G (MPa)	SIGF (kPa)
Core	35.4	8580	1125	0.49	1.50	6.00	10.50	37000	4.50	9.00
Mantle	38.8	1800	1274	0.49	3.67	14.70	18.30	18000	18.30	36.70
Cover	42.8	2040	950	0.49	10.50	42.00	-	-	-	-

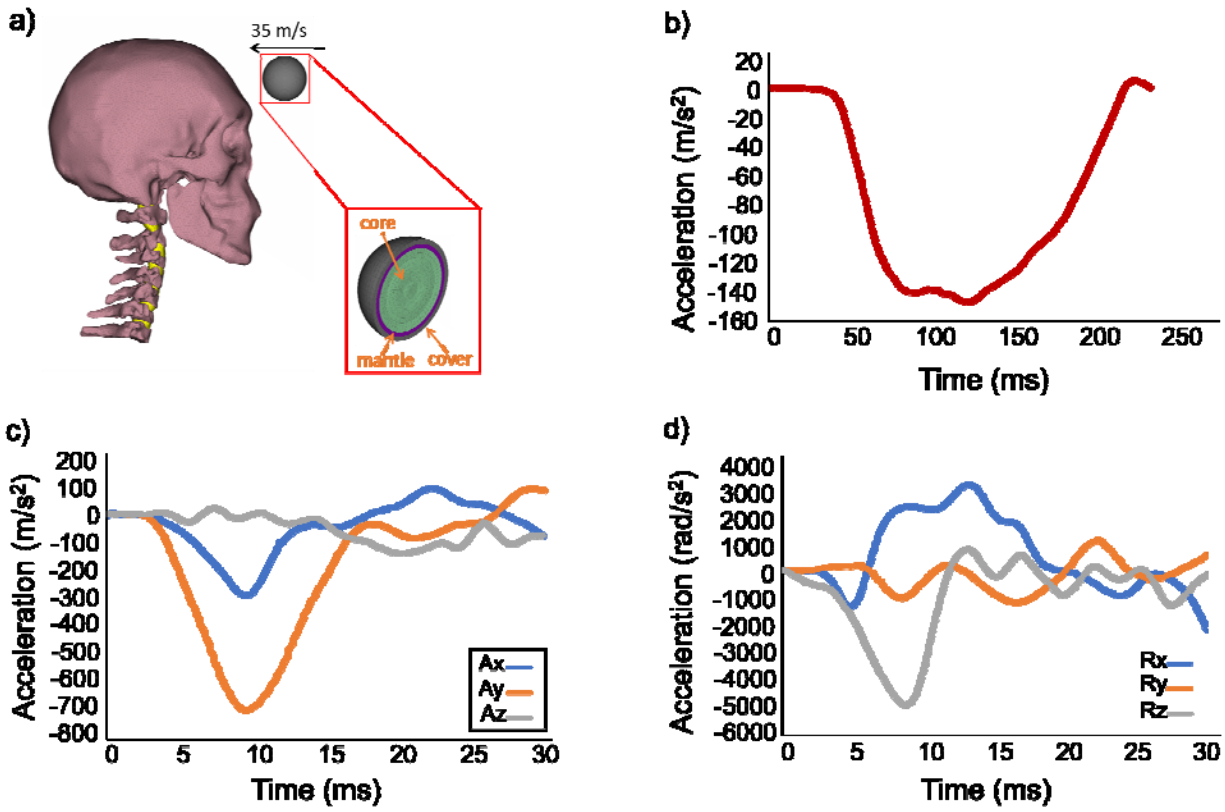

Fig. 1 Impact loads simulated in this study include: (a) Golf ball impact simulation (muscles, ligaments, and scalp are excluded from the figure for better visualization) [41], (b) Naval Biodynamics Laboratory (NBDL) study's linear acceleration profile [42], (c) Linear acceleration (Ax, Ay, Az) profiles, and (d) Rotational acceleration (Rx, Ry, Rz) profiles of helmet-to-helmet collisions in American football, taken from Zhang's study [43].

Study design

In order to examine the effects of neck muscle activations and neck damping characteristics on mechanical responses of the brain and the head-neck system, we considered three activation strategies across all neck muscles: 1) no-activation level, representing unprepared muscles experiencing an unanticipated impact scenario, 2) a low-to-medium activation level, indicating weak or inadequate muscle activation, and 3) high activation level, simulating tensed muscle conditions under anticipated impact scenarios. As previous research indicated that spinal muscles exhibit slight activity (approximately 5%) to provide stability to the spine (even when they are not actively contracting to provide any mobility), we applied a 5% activation level to all neck muscles during the no-activation level [46]. For second and third activation strategies, we provided varied activation levels to neck flexor and extensor muscle groups in order to simulate the realistic kinematic response of the head and neck system. In the Golf ball impact study, the flexor muscles play a crucial role in counteracting the frontal impact force. Therefore, for the low-to-medium activation level, we applied a 25% activation

level to the flexor muscles and 10% to the extensor muscles. Similarly, for the high activation level, we simulated tensed muscle conditions by using 80% flexor muscle activation and 10% extensor muscle activation.

In NBDL acceleration simulations, we applied a 25% activation level to extensor muscles and 10% to flexor muscles for the low-to-medium activation level as neck extensors are generally activated more than neck flexors in order to attenuate neck hyper-flexion. For the high activation level, we increased the extensor muscle activation to 80% while maintained the flexor muscle activation at 10%. In Zhang's combined linear and rotational acceleration scenarios, which do not strictly fall under pure neck flexion or extension, we applied same activation level to all neck flexor and extensor muscles throughout the impact duration. Specifically, we applied 25% activation level during the low-to-medium activation simulations and 80% during the high activation level simulation across all neck flexors and extensors.

The influence of neck damping on the risk of brain injury was examined by modeling the cervical intervertebral discs as hyper-elastic (low neck damping) and hyper-viscoelastic (high neck damping) properties. The hyper-elastic properties includes a nonlinear elastic module characterized by Mooney Rivlin hyper-elastic formulation [47, 48], whereas the hyper-viscoelastic properties include both the hyper-elastic component and a Prony series component to account for viscoelastic properties of the intervertebral discs [37]. We examined the effects of neck damping on the TBI mechanism by switching between hyper-elastic and hyper-viscoelastic material models of the intervertebral discs.

Injury estimation

Over time, researchers have made significant efforts to establish various injury criteria that can reliably predict the occurrence of brain injury. Initially, linear kinematics of the head were used as primary parameters in popular injury criteria like Head Injury Criterion (HIC) [49] and Gadd Severity Index (GSI) [50]. Later, it was found that the mechanical tolerance of brain tissues are poor against rotational acceleration and thus suggested to consider head rotational kinematics as another primary parameter in injury criterial formulation [51]. Consequently, alternative head injury criteria based on rotational kinematics were developed. For example, Takhounts et al. [51] devised brain injury criteria (BrIC) by correlating head rotational kinematics with brain strain. While the ease of measuring head kinematics made them a practical and popular option, the measurement of brain tissue deformation, such as maximal principal strain (MPS), has been proven to be more accurate and reliable measure of predicting brain injury, in particular, in diffuse brain injury scenarios [52, 53]. However, the measurement of brain MPS requires FE-based computational models, and is infeasible to assess in experimental studies [14]. As a result, the HIC [49] has been widely used as a TBI predictive metric (Equation 3) in both experimental and computational studies.

$$HIC = max\left(\left[\frac{1}{t_2 - t_1}\int_{t_1}^{t_2} a(t)dt\right]^{2.5}(t_2 - t_1)\right) \quad (3)$$

The variable, t represents time in milliseconds (ms), while a(t) denotes the linear acceleration profile measured in g's. The HIC quantifies the maximum value of the average acceleration over a specific time duration, raised to the power of 2.5 and multiplied by the duration itself. It is recommended to impose a limit on the time duration to enhance the relevance of HIC. In this study, we adopted HIC_{15}, which restricts the time difference between t_2 and t_1 to a maximum of 15 ms. HIC_{15} is a widely implemented variant of HIC, known for its popularity and acceptance in the field.

As HIC does not consider the rotational kinematics of the head, the BrIC was also widely used [51] as an additional parameter for estimating brain injuries (Equation 4).

$$BrIC = \sqrt{\left(\frac{\omega_x}{\omega_{xC}}\right)^2 + \left(\frac{\omega_y}{\omega_{yC}}\right)^2 + \left(\frac{\omega_z}{\omega_{zC}}\right)^2} \quad (4)$$

In Equation 5, ω_x, ω_y, and ω_z denotes angular velocity in x, y, and z directions respectively. Conversely, ω_{xC}, ω_{yC}, and ω_{zC} stands for the critical value of these parameters. We adopted these critical values from the literature with values of 66.25, 56.45, and 42.87 rad/s for ω_{xC}, ω_{yC}, and ω_{zC} respectively [51]. Using these BrIC values, we can estimate the abbreviated injury scale (AIS) spanning from 1 to 5 [51].

$$p(AIS\ 1) = 1 - e^{-\left(\frac{BrIC - 0.523}{0.065}\right)^{1.8}} \quad (5)$$

$$p(AIS\ 2) = 1 - e^{-\left(\frac{BrIC - 0.523}{0.324}\right)^{1.8}} \quad (6)$$

$$p(AIS\ 3) = 1 - e^{-\left(\frac{BrIC - 0.523}{0.531}\right)^{1.8}} \quad (7)$$

$$p(AIS\ 4) = 1 - e^{-\left(\frac{BrIC - 0.523}{0.647}\right)^{1.8}} \quad (8)$$

$$p(AIS\ 5) = 1 - e^{-\left(\frac{BrIC - 0.523}{0.673}\right)^{1.8}} \quad (9)$$

Equations 5 – 9 indicate the formulations for estimating the probability of AIS1, AIS2, AIS3, AIS4, and AIS5 scales that respectively indicate minor, moderate, serious (not life-threatening), severe (life-threatening), and critical (survival uncertain) severity of brain injuries. Furthermore, as our biofidilic head-neck FE model allowed us to go beyond the aforementioned kinematics-based injury metrics, we computed the brain's MPS in frontal, parietal, and occipital regions, alongside HIC and BrIC measures. We used the LS-DYNA (Livermore Software Technology Corporation, USA) explicit solver for conducting all impact simulations. These simulations were executed on the high-performance computing center located at our university. The computing center boasts cutting-edge infrastructure, including two AMD EPYC 7702 CPUs and 500 GB of memory per node, which provided ample computational resources to meet the demands of our simulations. Following the completion of the simulations, we performed the postprocessing of the results using META (BETA CAE Systems SA, Greece) and

MATLAB R2021b (MathWorks, USA). This combination of software tools allowed us to effectively analyze and interpret the obtained data.

Results

Analysis of HIC and BrIC Values

In both Golf ball impact and NBDL study simulations, the increase in muscle activation consistently led to a decrease in HIC and BrIC (Fig. 2) values. In comparison to no-activation baseline, Golf ball impact simulation showed a decrease in in both HIC and BrIC values for both low-to-medium activation (HIC: 4% for both low and high damping; BrIC: 13% for high damping, and 11% for low neck damping) and high activation level (HIC: 7% for both low and high damping; BrIC: 25% for both low and high damping). In NBDL simulations, while compared to the no-activation level, the reductions in HIC values were more substantial for both low-to-medium (HIC: 64% for high damping, and 67% for low neck damping; BrIC: 3% for high damping, and 5% for low neck damping) and high activation levels (HIC: 67% for high damping, and 69% for low neck damping; BrIC: 8% for high damping, and 9% for low neck damping). On the contrary, both HIC and BrIC values exhibited interesting trends in Zhang's study simulations. At first, the change in muscle activation from no-activation to low-to-medium levels decreased the HIC values by about 83% (high neck damping) and 74% (low neck damping) and the BrIC values by about 27% (regardless of the neck damping). Then, a drastic increase in HIC values (about 507% with high and 288% with low neck damping) and a moderate increase in BrIC values (about 25% with high and 1% with low neck damping) were observed with the increased muscle activation from low-to-medium to high activation levels.

The change in neck damping from low to high consistently showed decreasing trends of HIC and BrIC (Fig. 2) values across all simulations. In particular, Zhang's study simulations exhibited a substantial impact of neck damping (about 9%, 40%, and 6% reductions in HIC values and about 39%, 40%, and 25% reductions in BrIC values for no-activation, low-to-medium, and high activation levels, respectively). The NBDL study simulations revealed moderate impacts of neck damping – approximately 8%, 1%, and 3% reductions in HIC values and 5%, 3%, and 4% reductions in BrIC values for no-activation, low-to-medium, and high muscle activation levels, respectively. In contrast, the effect of neck damping in Golf ball impact simulations showed a trivial change in HIC values (about 1% reduction) but a moderate change in BrIC values (about 26% reduction) across all muscle activation levels.

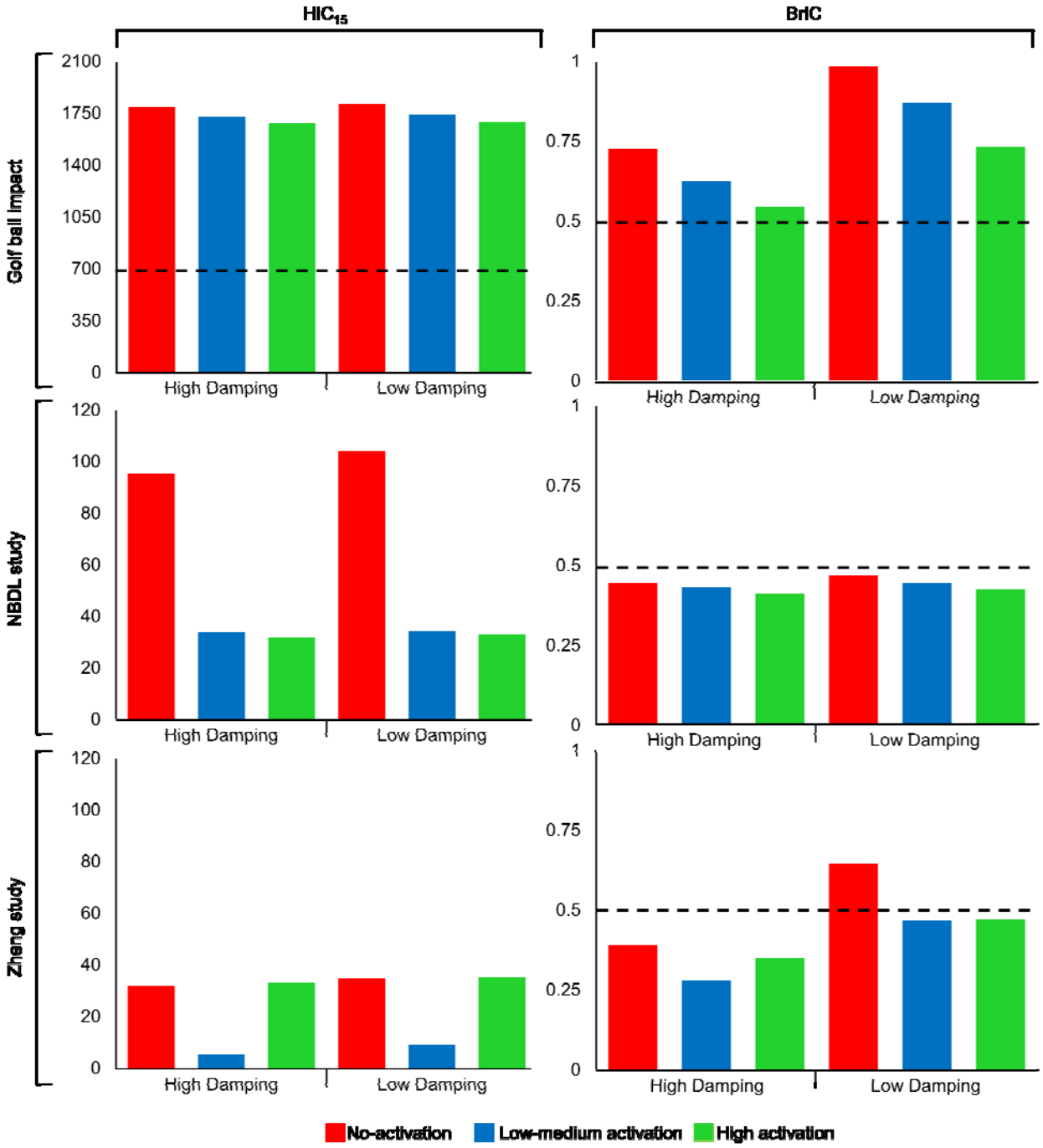

Fig. 2 Comparative analysis of HIC_{15} and BrIC in three simulated scenarios—Golf ball impact, NBDL's linear acceleration, and Zhang's combined rotational and linear acceleration simulations—for two neck damping—low (hyper-elastic) and high (hyper-viscoelastic)—properties and three muscle activation levels: 1) no-activation (unprepared muscles), 2) low-to-medium activation (weak or inadequate muscle activation), and 3) high activation (simulating tensed muscles). The dashed line indicates the injury threshold level.

Analysis of Brain MPS Results

In both Golf ball impact and NBDL study (Fig. 3) simulations, the brain MPS in frontal, parietal, and occipital regions consistently decreased with an increase in muscle activation level and neck damping. The most notable reductions were observed in the occipital region – about 17% (high neck damping) and 6% (low neck damping) for low-to-medium activation level and 18% (high neck damping) and 19% (low neck damping) for high activation level for Golf ball impact simulations and approximately 27% (high neck damping) and 29% (low neck damping) for low-to-medium activation level and 50% (high neck damping) and 41% (low neck damping) for high activation level in NBDL study simulations, compared to the no-activation level.

In Zhang's study simulations, similar to HIC and BrIC results, the brain MPS in all three regions notably decreased with the change in muscle activation from the no-activation to low-to-medium activation levels, but increased from the low-to-medium to high activation levels (Fig. 3). In the frontal region, we observed a decrease of about 19% (high neck damping) and 84% (low neck damping) at low-to-medium activation level compared to no-activation level and, conversely, an increase of about 73% (high neck damping) and 18% (low neck damping) at high activation level than the low-to-medium activation levels. In the parietal region, there was a decrease of about 26% with high and 48% with low neck damping at low-to-medium activation level compared to no-activation level an increase of about 84% with high and 17% with low neck damping at high activation level than the low-to-medium activation level. In the occipital region, the increased muscle activity from no-activation to low-to-medium activation levels reduced the brain MPS by about 90% (high damping) and 60% (low neck damping) and increased by about 305% (high damping) and 23% (low damping) with from the low-to-medium to high activation levels. The increase in neck damping reduced the brain MPS by approximately 83%, 28%, and 1% at no-activation and increased them by about 18%, 38%, and 19% at low-to-medium, along with around 19%, 12%, and 63% at high activation levels at frontal, parietal, and occipital regions, respectively.

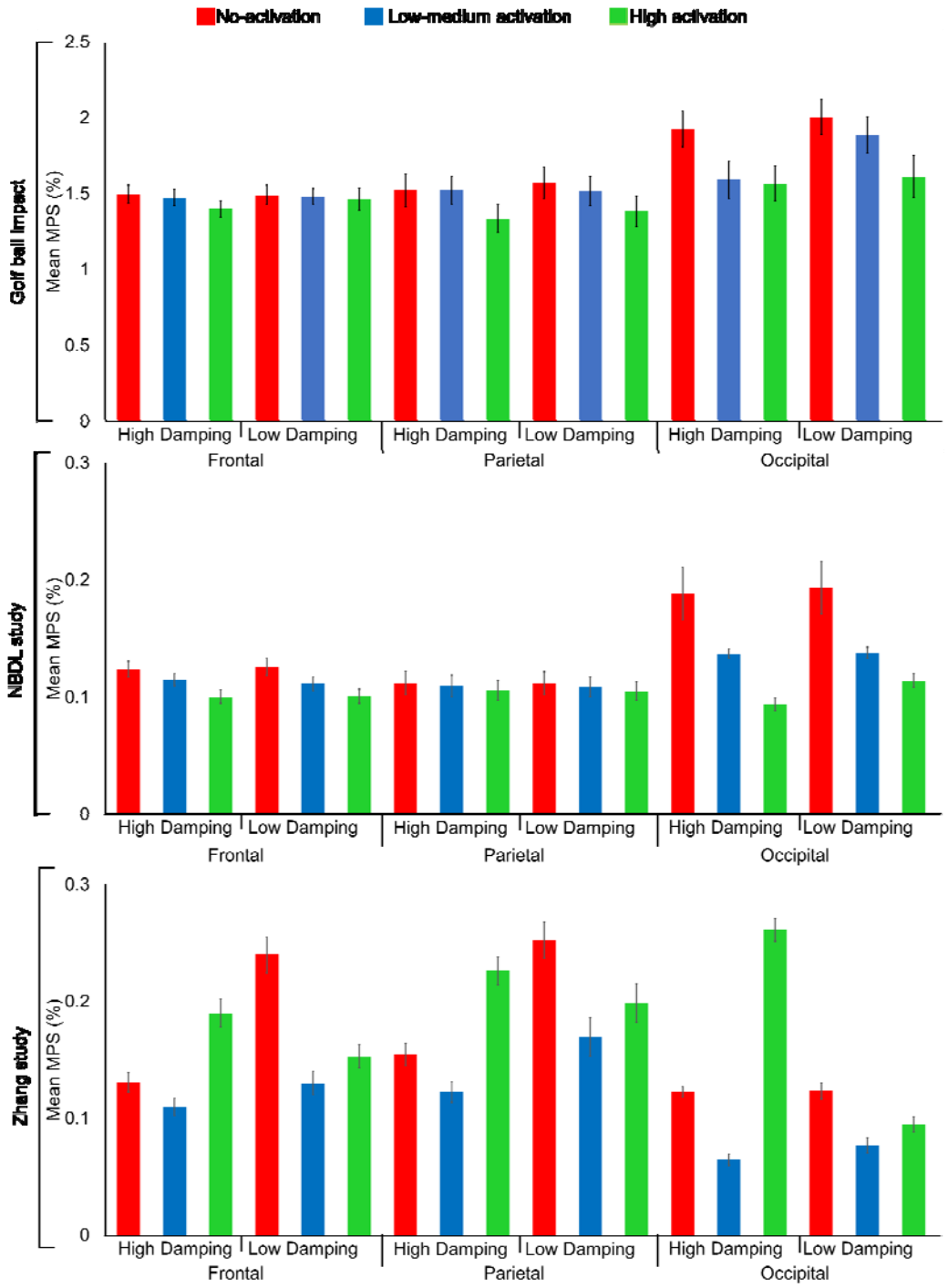

Fig. 3 Comparative analysis of the brain maximum principle strain (MPS) (mean ± standard error) at three frontal, parietal, and occipital regions under three muscle activation levels—1) no-activation (unprepared muscles), 2) low-to-medium activation (weak or inadequate muscle activation), and 3) high activation (simulating tensed muscles)—and for two neck damping—low (hyper-elastic) and high (hyper-viscoelastic)—properties in three simulated scenarios: Golf ball impact, NBDL's linear acceleration, and Zhang's combined rotational and linear acceleration simulations.

Probability of TBI

In NBDL and Zhang's study simulations, the HIC and BrIC values remained below the injury threshold, except for one scenario (no-activation level, low neck damping) in Zhang's study wherein the probable risks of AIS1, AIS2, AIS3, AIS4, and AIS5 based on BrIC values were about 98.54%, 20.71%, 9.11%, 6.45%, and 6.04%, respectively. On the contrary, both HIC and BrIC values showed the risk of TBIs in all scenarios of Golf ball impact study (Fig. 3). Therefore, we only estimated the AIS 1 – 5 for the Golf ball impact simulations. As shown in Fig. 4, the AIS values of Golf ball impact simulations showed a trend of reduced probability of TBI with the increase in muscle activation. This reduction was particularly large with higher neck damping (about 4% for AIS 1 and 60% for AIS 2-5 at the low-to-medium activation level and about 69% for AIS 1 and 96% for AIS 2-5 at the high activation level) than the lower neck damping (about 1% for AIS 1, 16% for AIS 2, and roughly 30% for AIS 3-5 at the low-to-medium activation level and about 1% for AIS 1, 50% for AIS 2, and 65% for AIS 3-5 for the high activation level).

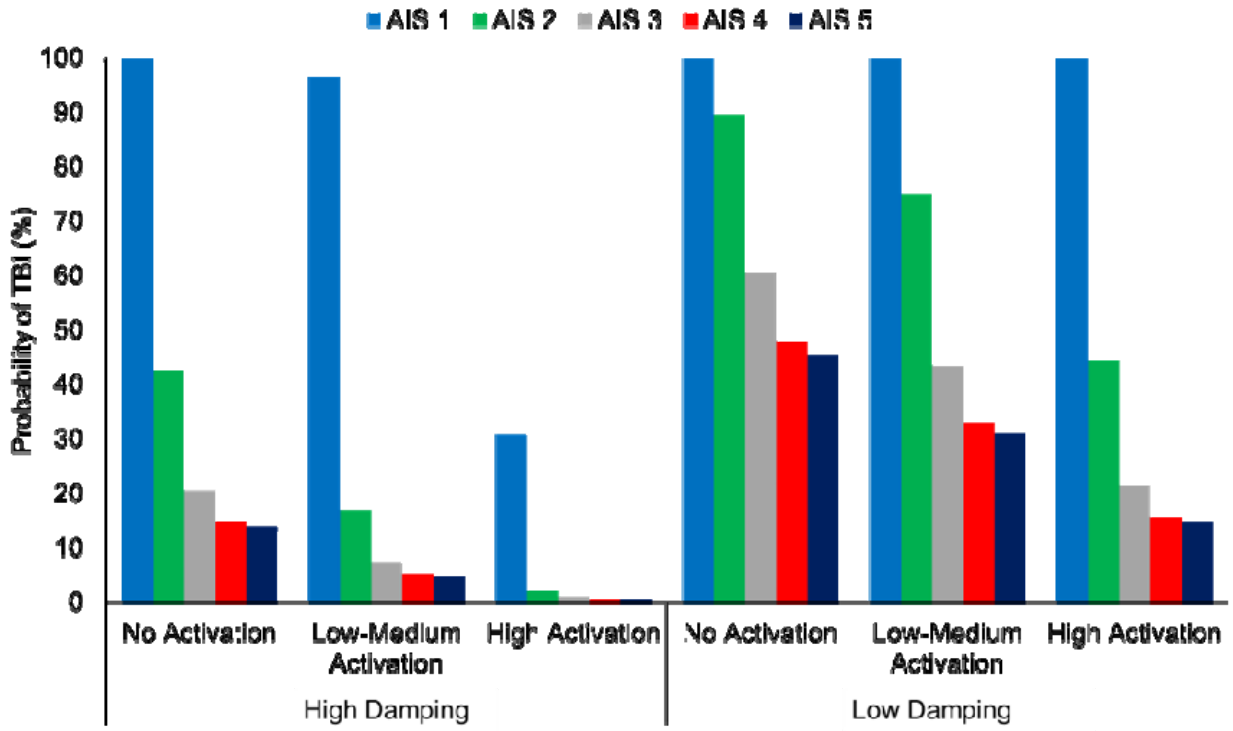

Fig. 4 Probability of traumatic brain injury (TBI) assessed using abbreviated injury scale (AIS) for the Golf ball impact simulations. AIS1, AIS2, AIS3, AIS4, and AIS5 indicate minor, moderate, serious (not life-threatening), severe (life-threatening), and critical (survival uncertain) severity of injuries, respectively.

Discussion

We aimed to study the impacts of neck muscle activation and neck damping on TBI outcomes for three impact scenarios—1) direct impact (Golf ball impact study), 2) pure linear acceleration (NBDL study), and 3) combined linear and rotational acceleration (Zhang's study)—in order to deepen our understanding of the roles of neck structures in TBI mechanics. Our results demonstrated the impacts of both neck muscle activation and neck damping on HIC, BrIC, and brain MPS injury metrics across all simulated scenarios.

During head-neck impacts, the impact energy (forces) transmitted through the scalp, skull, and CSF to the brain can cause brain structural deformation. Neck muscles play a key role in attenuating this impact force. The level of this impact attenuation by neck muscles depends on their activation level, position, timing, and designated roles [11, 54]. For example, neck flexor muscles play a crucial role in counteracting the external impact forces in instances like the direct impact of a Golf ball on the forehead. On the other hand, in high acceleration scenarios like NBDL or Zhang's helmet-to-helmet impacts, neck extensor muscles play a vital role in reducing neck hyper-flexion (in NBDL simulations), whereas neck rotator muscles contribute to reducing rapid neck rotational acceleration (in Zhang's scenarios). The coordinated actions of these neck muscles also contribute to reducing the brain-skull relative motion. Consequently, across all NBDL and Golf ball impact simulations, our results exhibited a consistent pattern of reduced TBI metrics with the increase in neck muscle activation, which align well with prior experimental [20, 55] and FE-based computational studies [11, 17]. Furthermore, the increase in neck muscle activation resulted in reduced brain deformation in both frontal (coup) and occipital (countercoup) regions, suggesting that the strengthening of neck muscles through targeted training could be a crucial strategy in reducing the risk and severity of brain injuries in various impact scenarios. It also highlights the importance of the inclusion of neck muscles while investigating the TBI mechanism using both experimental and computational methods.

The brain selects the most appropriate muscles and varied activation levels (i.e., muscle activation strategies) to achieve a specific motor goal or movement. In Zhang's linear and rotational acceleration scenarios, it was observed that increasing muscle activation from no-activation (5%) level to low-to-medium activation level (25%) resulted in a reduction in all brain injury metrics. However, when the muscle activation level was increased to the high muscle activation level (80%), there was a drastic increase in brain injury metrics. This inconsistent pattern revealed two unprecedented insights. First, a simple muscle activation strategy, which involved uniformly applying high activations (80%) across flexor, extensor, and rotator muscles, might result in abnormally high joint reaction forces to the skull, which, in turn, can cause increased brain-skull movement. A more sophisticated and accurate muscle activation strategy, such as modeling the rotator muscles with a higher activation than the flexor or extensor muscle groups, might have consistently provided reduced brain injury metrics.

Therefore, it is essential to model neck muscles with scenario-specific precise muscle activation strategies in order to obtain an accurate understanding of TBI mechanism. Secondly, athletes with a history of concussion, who typically exhibit abnormal muscle activation strategies, are at a higher risk of experiencing recurring TBI or other musculoskeletal injuries [56]. Thus, our findings underscored the importance of neck muscle activation strategies (i.e., motor function) in TBI study.

In this study, we perturbed neck damping by altering the viscoelastic properties of intervertebral discs in order to investigate the resulting changes in the brain's mechanical response. Like mechanical dampers, higher damping characteristics of the neck are expected to absorb more impact energy as it leads to a greater phase difference between impact force and tissue response instances. Previous research [12] showed that increasing neck damping in a direct head impact reduces the adverse mechanical responses of the brain. Our findings align with this, demonstrating that neck damping leads to a reduction in brain injury metrics. Therefore, it is essential to model intervertebral discs with appropriate damping characteristics in order for an accurate and comprehensive understanding of the TBI mechanism. Interestingly, the reductions in brain injury metrics were more prominently observed in brain MPS, followed by BrIC, than HIC in all simulated scenarios. This could be due to the fact that MPS directly reflects the mechanical deformation (strain) of brain tissues and BrIC accounts for rotational head kinematics, whereas HIC is limited to linear head kinematics [57]. Though the brain MPS is a more reliable measure of TBI, it requires computational brain models, thus posing practical challenges in many applications. In contrast, both HIC and BrIC are kinematics-based metrics. Especially, owing to its ease-of-use in estimating a range of TBI severities (AIS 1 to 5) and the ability to capture the brain's response to rotational accelerations or shear forces, BrIC has recently become a popular injury metrics in many field (both engineering and clinical settings) applications.

This study has several limitations. Although we modeled three scenarios to study TBI mechanisms, it is essential to acknowledge that our study did not encompass all head impact types. Future investigations should explore a broader range of impacts, especially rear and side impact scenarios, to enhance our understanding of the neck's role in TBI mechanisms. Additionally, we assessed TBI using three commonly used injury metrics. The inclusion of other off-the-shelf TBI injury metrics could have provided a more comprehensive TBI assessment. Moreover, we examined the neck damping characteristics by perturbing the damping properties of cervical intervertebral discs. This may not fully capture the total neck damping properties as cervical muscles, ligaments, tendons, and other soft tissues also contribute to neck damping. Thence, future research should account their combined contribution to TBI mitigation. Furthermore, we attempted only three simplistic muscle activation strategies by separating neck muscles into two groups (flexor and extensor muscles). This may not fully reflect the intricate motor activation strategies governed by the brain. Furthermore, it's essential to recognize that muscle activation strategies and neck properties are influenced by various factors, including brain impairments, age-related changes, and sports-related

injuries. These factors should be taken into account in future research to understand the TBI mechanics of people with a history of those changes or disorders. Finally, we model each intervertebral disc as a single solid body, neglecting the inherent composition of annulus fibrosis and nucleus pulposus with distinct mechanical properties.

Despite these limitations, our study reveals the crucial role played by neck muscles and neck damping in mitigating the severity of brain injury during traumatic head impacts. The knowledge gained from this study has practical applications. These include the development of tailored neck strength training protocols to enhance the mechanical capacity of neck muscles and motor strategies, as well as the design of protective equipment for those at higher risk of neck injuries, with the purpose of reducing the likelihood of TBI during mechanical impacts.

Acknowledgments

This work was primarily supported by the National Science Foundation (**2239110**). We thank Felipe Santos, Leonardo Wei, and Gustavo Paulon for their assistance in data processing and finite element model development.

Declarations

Conflict of Interest: The authors declare that there is no conflict of interest.

References

1. Menon DK, Schwab K, Wright DW, Maas AI. Position statement: definition of traumatic brain injury. Archives of physical medicine and rehabilitation. 2010;9111:1637-40.
2. Prevention CfDCa. National Center for Health Statistics: Mortality Data on CDC WONDER [Available from: https://wonder.cdc.gov/mcd.html.
3. Daugherty J, Waltzman D, Sarmiento K, Xu L. Traumatic brain injury–related deaths by race/ethnicity, sex, intent, and mechanism of injury—United States, 2000–2017. Morbidity and Mortality Weekly Report. 2019;6846:1050.
4. Miller GF, Kegler SR, Stone DM. Traumatic brain injury–related deaths from firearm suicide: United States, 2008–2017. American journal of public health. 2020;1106:897-9.
5. Prevention CfDCa. National Center for Injury Prevention and Control.
6. Gordon KE, Dooley JM, Wood EP. Descriptive epidemiology of concussion. Pediatric neurology. 2006;345:376-8.
7. Selassie AW, Wilson DA, Pickelsimer EE, Voronca DC, Williams NR, Edwards JC. Incidence of sport-related traumatic brain injury and risk factors of severity: a population-based epidemiologic study. Annals of epidemiology. 2013;2312:750-6.
8. Sarmiento K, Thomas KE, Daugherty J, Waltzman D, Haarbauer-Krupa JK, Peterson AB, et al. Emergency department visits for sports-and recreation-related traumatic brain injuries among children—United States, 2010–2016. Morbidity and Mortality Weekly Report. 2019;6810:237.

9. Zasler ND, Katz DI, Zafonte RD. Brain injury medicine: principles and practice: Demos Medical Publishing; 2012
10. Andriessen TM, Jacobs B, Vos PE. Clinical characteristics and pathophysiological mechanisms of focal and diffuse traumatic brain injury. Journal of cellular and molecular medicine. 2010;1410:2381-92.
11. Jin X, Feng Z, Mika V, Li H, Viano DC, Yang KH. The role of neck muscle activities on the risk of mild traumatic brain injury in American football. Journal of biomechanical engineering. 2017;13910.
12. Dirisila V, Karami G, Ziejewski M, editors. The effects of neck stiffness properties on brain response under impact loads. ASME International Mechanical Engineering Congress and Exposition; 2010.
13. Bailey AM, Sherwood CP, Funk JR, Crandall JR, Carter N, Hessel D, et al. Characterization of concussive events in professional American football using videogrammetry. Annals of biomedical engineering. 2020;4811:2678-90.
14. Tierney G. Concussion biomechanics, head acceleration exposure and brain injury criteria in sport: a review. Sports biomechanics. 2022:1-29.
15. Funk JR, Jadischke R, Bailey A, Crandall J, McCarthy J, Arbogast K, Myers B. Laboratory reconstructions of concussive helmet-to-helmet impacts in the National Football League. Annals of biomedical engineering. 2020;48:2652-66.
16. King AI, Ruan J, Zhou C, Hardy WN, Khalil T. Recent advances in biomechanics of brain injury research: a review. Journal of neurotrauma. 1995;124:651-8.
17. Bruneau DA, Cronin DS. Head and neck response of an active human body model and finite element anthropometric test device during a linear impactor helmet test. Journal of Biomechanical Engineering. 2020;1422.
18. Ji S, Ghajari M, Mao H, Kraft RH, Hajiaghamemar M, Panzer MB, et al. Use of brain biomechanical models for monitoring impact exposure in contact sports. Annals of Biomedical Engineering. 2022;5011:1389-408.
19. Reber JG, Goldsmith W. Analysis of large head-neck motions. Journal of Biomechanics. 1979;123:211-22.
20. Eckner JT, Oh YK, Joshi MS, Richardson JK, Ashton-Miller JA. Effect of neck muscle strength and anticipatory cervical muscle activation on the kinematic response of the head to impulsive loads. The American journal of sports medicine. 2014;423:566-76.
21. Winters JM. Hill-based muscle models: a systems engineering perspective. Multiple muscle systems: biomechanics and movement organization: Springer; 1990. p. 69-93.
22. Tierney RT. Gender differences in head-neck segment dynamic stabilization during head acceleration: Temple University; 2004
23. Collins CL, Fletcher EN, Fields SK, Kluchurosky L, Rohrkemper MK, Comstock RD, Cantu RC. Neck strength: a protective factor reducing risk for concussion in high school sports. The journal of primary prevention. 2014;35:309-19.
24. Schmidt JD, Guskiewicz KM, Blackburn JT, Mihalik JP, Siegmund GP, Marshall SW. The influence of cervical muscle characteristics on head impact biomechanics in football. The American journal of sports medicine. 2014;429:2056-66.
25. Mihalik JP, Guskiewicz KM, Marshall SW, Greenwald RM, Blackburn JT, Cantu RC. Does cervical muscle strength in youth ice hockey players affect head impact biomechanics? Clinical journal of sport medicine. 2011;215:416-21.
26. Mansell J, Tierney RT, Sitler MR, Swanik KA, Stearne D. Resistance training and head-neck segment dynamic stabilization in male and female collegiate soccer players. Journal of athletic training. 2005;404:310.
27. Bahreinizad H, Chowdhury SK, Wei L, Paulon G, Santos F. Development and Validation of an MRI-Derived Head-Neck Finite Element Model. bioRxiv. 2023:2023.02. 12.528203.

28. Winters JM. Hill-based muscle models: a systems engineering perspective. Multiple muscle systems: biomechanics and movement organization. 1990:69-93.
29. Dahl MC, Rouleau JP, Papadopoulos S, Nuckley DJ, Ching RP. Dynamic characteristics of the intact, fused, and prosthetic-replaced cervical disk. 2006.
30. Mao H, Zhang L, Jiang B, Genthikatti VV, Jin X, Zhu F, et al. Development of a finite element human head model partially validated with thirty five experimental cases. Journal of biomechanical engineering. 2013;13511:111002.
31. Salimi Jazi M, Rezaei A, Azarmi F, Ziejewski M, Karami G. Computational biomechanics of human brain with and without the inclusion of the body under different blast orientation. Computer methods in biomechanics and biomedical engineering. 2016;199:1019-31.
32. Tuchtan L, Godio-Raboutet Y, Delteil C, Léonetti G, Marti M-DP, Thollon L. Study of cerebrospinal injuries by force transmission secondary to mandibular impacts using a finite element model. Forensic science international. 2020;307:110118.
33. Tse KM, Tan LB, Lim SP, Lee HP. Conventional and complex modal analyses of a finite element model of human head and neck. Computer methods in biomechanics and biomedical engineering. 2015;189:961-73.
34. Cotton R, Pearce CW, Young PG, Kota N, Leung A, Bagchi A, Qidwai S. Development of a geometrically accurate and adaptable finite element head model for impact simulation: the Naval Research Laboratory–Simpleware Head Model. Computer methods in biomechanics and biomedical engineering. 2016;191:101-13.
35. Ramzanpour M, Hosseini-Farid M, McLean J, Ziejewski M, Karami G. Visco-hyperelastic characterization of human brain white matter micro-level constituents in different strain rates. Medical & Biological Engineering & Computing. 2020;58:2107-18.
36. Bennion NJ, Zappalá S, Potts M, Woolley M, Marshall D, Evans SL. In vivo measurement of human brain material properties under quasi-static loading. Journal of the Royal Society Interface. 2022;19197:20220557.
37. Castro A, Paul C, Detiger S, Smit T, Van Royen B, Pimenta Claro J, et al. Long-term creep behavior of the intervertebral disk: comparison between bioreactor data and numerical results. Frontiers in Bioengineering and Biotechnology. 2014;2:56.
38. Panzer MB, Fice JB, Cronin DS. Cervical spine response in frontal crash. Medical engineering & physics. 2011;339:1147-59.
39. Winters JM. Hill-based muscle models: a systems engineering perspective. Multiple muscle systems: Springer; 1990. p. 69-93.
40. Zhang QH, Teo EC, Ng HW. Development and validation of a C0–C7 FE complex for biomechanical study. 2005.
41. Li Y, Gao X-L. Modeling of head injuries induced by golf ball impacts. Mechanics of Advanced Materials and Structures. 2019;2621:1751-63.
42. Ewing CL, Thomas DJ. Human Head and Neck Response to Impact Acceleration. Naval Aerospace Medical RESEARCH Lab Pensacola Fl; 1972.
43. Zhang L, Yang KH, King AI. A proposed injury threshold for mild traumatic brain injury. J Biomech Eng. 2004;1262:226-36.
44. Ma X, Aravind A, Pfister BJ, Chandra N, Haorah J. Animal models of traumatic brain injury and assessment of injury severity. Molecular neurobiology. 2019;56:5332-45.
45. Thunnissen J, Wismans J, Ewing C, Thomas D. Human volunteer head-neck response in frontal flexion: a new analysis. SAE transactions. 1995:3065-86.
46. Szeto GPY, Straker LM, O'Sullivan PB. Neck–shoulder muscle activity in general and task-specific resting postures of symptomatic computer users with chronic neck pain. Manual Therapy. 2009;143:338-45.
47. Ogden RW. Non-linear elastic deformations: Courier Corporation; 1997

48. Rivlin RS. Large elastic deformations of isotropic materials IV. Further developments of the general theory. Philosophical transactions of the royal society of London Series A, Mathematical and physical sciences. 1948;241835:379-97.
49. Hutchinson J, Kaiser MJ, Lankarani HM. The head injury criterion (HIC) functional. Applied mathematics and computation. 1998;961:1-16.
50. Gadd CW. Use of a weighted-impulse criterion for estimating injury hazard. SAE technical paper; 1966. Report No.: 0148-7191.
51. Takhounts EG, Craig MJ, Moorhouse K, McFadden J, Hasija V. Development of brain injury criteria (BrIC). SAE Technical Paper; 2013.
52. Wright RM, Ramesh K. An axonal strain injury criterion for traumatic brain injury. Biomechanics and modeling in mechanobiology. 2012;11:245-60.
53. Donat CK, Yanez Lopez M, Sastre M, Baxan N, Goldfinger M, Seeamber R, et al. From biomechanics to pathology: predicting axonal injury from patterns of strain after traumatic brain injury. Brain. 2021;1441:70-91.
54. Fanton M, Kuo C, Sganga J, Hernandez F, Camarillo DB. Dependency of head impact rotation on head-neck positioning and soft tissue forces. IEEE Transactions on Biomedical Engineering. 2018;664:988-99.
55. Choi W, Robinovitch S, Ross S, Phan J, Cipriani D. Effect of neck flexor muscle activation on impact velocity of the head during backward falls in young adults. Clinical biomechanics. 2017;49:28-33.
56. Bussey M, McLean M, Pinfold J, Anderson N, Kiely R, Romanchuk J, Salmon D. History of concussion is associated with higher head acceleration and reduced cervical muscle activity during simulated rugby tackle: an exploratory study. Physical therapy in sport. 2019;37:105-12.
57. Kleiven S. Why most traumatic brain injuries are not caused by linear acceleration but skull fractures are. Frontiers in bioengineering and biotechnology. 2013;1:15.
58. Zhan X, Li Y, Liu Y, Domel AG, Alizadeh HV, Raymond SJ, et al. The relationship between brain injury criteria and brain strain across different types of head impacts can be different. Journal of the Royal Society Interface. 2021;18179:20210260.